Title	A novel fine-tuning mesoporous adsorbent for simultaneous lead(II) detection and removal from wastewater
Author(s)	Md. Rabiul Awal, Md. Munjur Hasan
Citation	Sensors and Actuators B: Chemical, 202, pp.395-403
Text Version	Author
URL	http://jolissrch-inter.tokai-sc.jaea.go.jp/search/servlet/search?5045768
DOI	http://dx.doi.org/10.1016/j.snb.2014.05.103
Right	This is the author's version of a work that was accepted for publication in Sensors and Actuators B: Chemical. Changes resulting from the publishing process, such as peer review, editing, corrections, structural formatting, and other quality control mechanisms, may not be reflected in this document. Changes may have been made to this work since it was submitted for publication. A definitive version was subsequently published in Sensors and Actuators B: Chemical, vol.202, 31 Oct 2014, DOI: 10.1016/j.snb.2014.05.103.

A novel fine-tuning mesoporous adsorbent for simultaneous lead(II) detection and removal from wastewater

Md. Rabiul Awual [a]****, Md. Munjur Hasan*** [b]

[a] *Actinide Coordination Chemistry Group, Quantum Beam Science Directorate, Japan Atomic Energy Agency (SPring–8), Hyogo 679–5148, Japan*

[b] *Shaheed Ziaur Rahman Medical College, Bogra 5800, Bangladesh*

***** Corresponding author. Tel.: +81 791 58 2642; fax: +81 791 58 0311.
E–mail address: awual75@yahoo.com; awual.rabiul@jaea.go.jp (M. R. Awual).

Research highlights:

- Novel mesoporous adsorbent was prepared for ultra-trace Pb(II) ions capturing.
- Mesoporous adsorbent can be removed the Pb(II) with high sensitivity and selectivity.
- Adsorbent has reusability in many cycles without deterioration in its performance.

Graphical Abstract

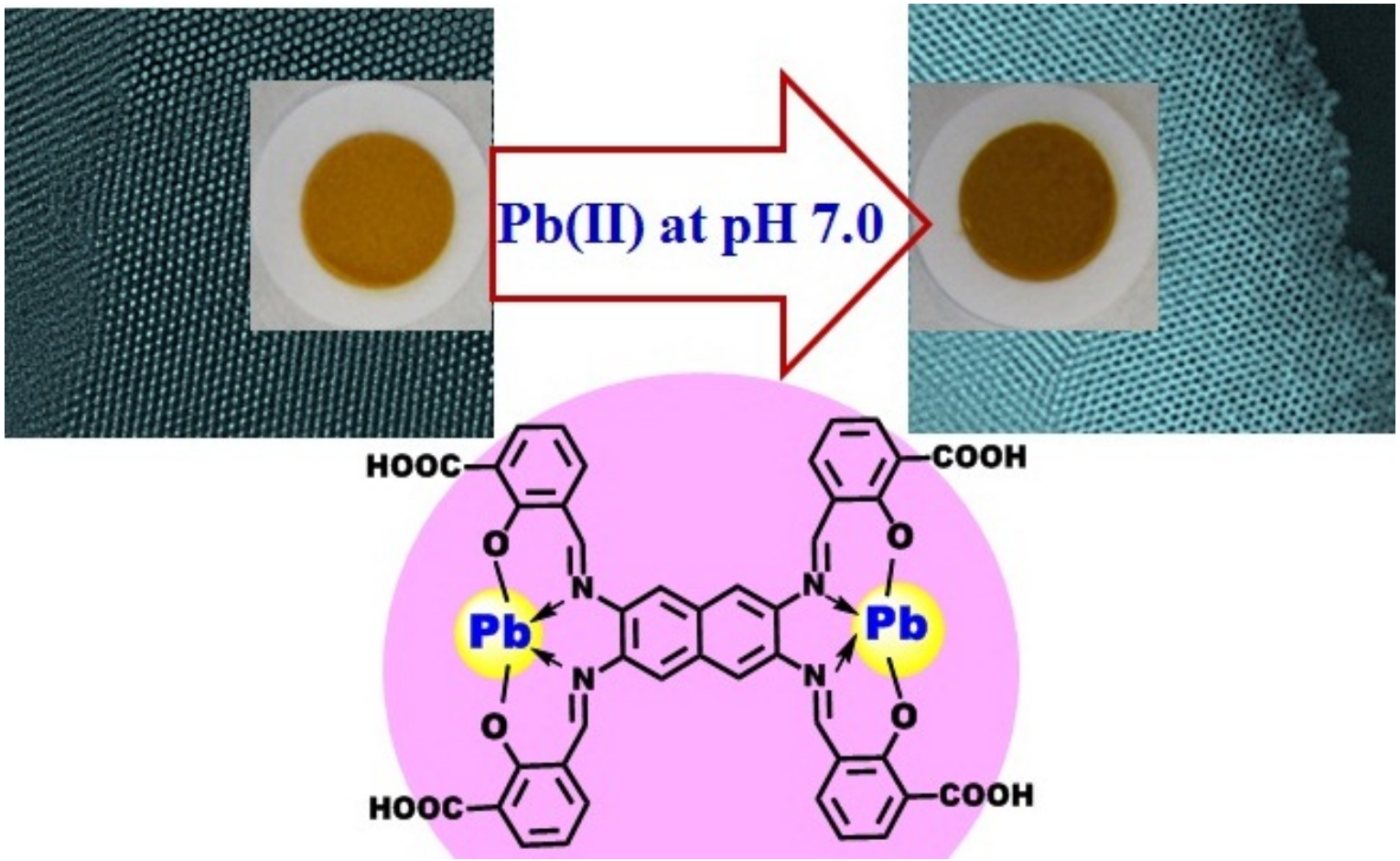

A B S T R A C T

The functionalized mesoporous silica based fine-tuning mesoporous adsorbent was developed for ultra-trace lead (Pb(II)) detection and removal from wastewater. The mesoporous adsorbent was fabricated by direct immobilization of 1E,1`E,1``E,1```E(tetrakis(3-carboxysalicylidene)) naphthalene–1,2,5,5–tetramine (TSNT) onto mesoporous silica monoliths. The design of the ligand into ordered pore-based mesoporous adsorbent transformed the Pb(II) detection and removal systems into smart and stable assemblies. The ability of the mesoporous adsorbent to detect and remove Pb(II) from aqueous solutions has been studied and discussed with different optimized conditions of concentrations, the amount of mesoporous adsorbent, concentration of coexisting electrolyte and pH. The design of such a tunable mesoporous adsorbent offered a simple procedure in such toxic Pb(II) ions removal without using high-tech, sophisticated instruments. The mesoporous adsorbent was able to detect the ultra-trace Pb(II) ions with high sensitivity and selectivity based on charge transfer ((intense π–π transition) transduction. Therefore, the mesoporous adsorbent proved to have an efficient ability for continuous monitoring of toxic Pb(II) ions even on-site and in situ chemical analyses. The removal data revealed that mesoporous adsorbent has high sorption capacity (184.32 mg/g) based on sorption isotherms measurements. The major advantage of the tunable design mesoporous adsorbent was that the mesoporous adsorbent retained highly efficient sensitive selectivity without a significant kinetic hindrance, despite the slight decrease of sorption after several regeneration/reuse cycles. Uptake of Pb(II) onto mesoporous adsorbent to equilibrium occurred quickly and the mesoporous adsorbent could be regenerated for reuse with diluted HCl. Therefore, the mesoporous adsorbent has been shown to have the potential to be used as an effective adsorbent for ultra–trace Pb(II) ions detection and removal from wastewater.

Keywords: Pb(II) ions; Mesoporous adsorbent; Mesostructures; Selective detection and removal; Reuses.

1. Introduction

Tons of heavy metals are generated annually by industrial activity that has contaminated water bodies all over the world. Therefore, heavy metal pollution has received much attention in the media and scientific literature due to the severe toxic effects on human health and the environment [**1**]. However, lead (Pb(II)) is generated from the paints, pigments and printing industries, petroleum refining industry, use of storage batteries and electrodes in electrochemistry and chemical industries [**2–4**]. Lead is the second top priority hazardous substance according to ATSDR [**5**]. Lead is non-biodegradable and has a tendency to accumulate in blood, soft tissues and as lead triophosphate in bones. Long-term consumption of water containing Pb(II), even in low concentration, can cause many chronic or acute diseases such as brain damage, kidney damage, and gastrointestinal distress to humans, as well as damage to the central nervous center, renal system, convulsions possibly resulting in death and mental retardation in children [**6–8**]. Therefore, the maximal permissible limit is set to 0.015 mg/L (15 ppb) [**9**]. This concentration value is considered as the threshold for the safeguard of public health and maintenance of an ecological equilibrium. Thus, monitoring of lead from the environment with high sensitivity and the removal of excess lead ions from wastewater is important and essential to safeguarding the public health and maintaining water quality.

Recent attention to the impact of low level Pb(II) on public health has encouraged a major research effort to develop effective means to detect and remove toxic Pb(II) from drinking water and wastewater. There are several techniques widely-used for Pb(II) detection such as atomic absorption spectrometry (AAS), colorimetric assay, atomic emission spectrometry (AES), electrochemistry methods, biosensors, nuclear magnet resonance, and inductively coupled plasma mass spectrometry (ICP-MS) [**10–13**]. However, most traditional analytical techniques do not allow direct analysis of Pb(II) especially in complex media and

their sophisticated instrumentation and/or complicated sample preparation hamper their application for in-field studies. For this reason, interest in innovative methods to monitor contaminated water has been increasing based on simple, robust, easy-to-use and efficient sensitivity. Therefore, a variety of chemosensors [**12**] have been developed to detect Pb(II) in wastewater. However, colorimetric methods [**13**] are attractive and able to be directly read with naked-eye observation. The colorimetric methods are quite sensitive, however, these are not specific for Pb(II) and form color complexes with other metal ions [**14–16**]. Therefore, an effective method for technological diversity is the optical mesoporous adsorbent model based on generating the analytical signal as a response to binding with Pb(II) ions.

Several technological methods such as chemical precipitation, coagulation, complexions, ion exchange, solvent extraction, reverse osmosis, distillation and adsorption have been used to remove Pb(II) from wastewater [**17–23**]. Many of them suffer from incomplete Pb(II) removal, high reagent and energy requirements and generation of toxic waste sludge products that require proper disposal and further treatment. In the last few decades, the adsorption process has received much attention and represents an effective process for the removal of pollutant contaminants [**24,25**]. Moreover, adsorption of solid adsorbents is more effective at low concentrations of harmful pollutants removal. However, the high price of adsorbents increases the cost of treatment methods. Therefore, several research efforts have been performed in order to develop new sensitive, selective and cost-effective adsorbents.

Recently, nanaomaterials based nanotechnology is gaining considerable public interest for ultra-trace toxic metal ions removal due to the high surface-area-to-volume ratio that makes them a suitable and cost-effective treatment method [**26–28**]. So, the present work is aimed at developing ligand supported mesoporous adsorbent for simultaneous low-level Pb(II) detection and removal from water. The conventional ligands are slow metal-ion capturing and lack selectivity toward a particular metal ion. So the specific and fast complexation of the metal

ions with ligand immobilized mesoporous adsorbent was investigated for selective removal of heavy-metal ions from wastewater.

In this study, we developed mesoporous adsorbent by successful immobilization of synthesized 1E,1`E,1``E,1```E (tetrakis(3-carboxysalicylidene))naphthalene-1,2,5,5-tetramine (TSNT) ligand (**Scheme 1**) onto large cage mesostructures silica for the detection and removal of Pb(II) ions. The ligand onto mesoporous silica was associated based on non-covalent interactions, Van der Waals forces and reversible covalent bonds. Several parameters such as pH, limit of detection, adsorbent dosage, contact time, and sorption capacity were systematically investigated and discussed. This paper is concerned with operational parameters for optimum detection and removal of Pb(II) from water by fine tunable mesoporous adsorbent. A complete laboratory investigation of this process would generally consist of three parts such as (i) preparation of mesoporous adsorbent, (ii) demonstration the detection operation and feasibility low detection limit and (iii) optimum removal operation to obtain data to be used in designing the full-scale plant.

2. Materials and methods

2.1. Materials

All materials and chemicals were of analytical grade and used as purchased without further purification. Tetramethylorthosilicate (TMOS) and the triblock copolymers of poly(ethylene oxide–b–propylene oxide–b–ethylene oxide) as Pluronic F108, designated as F108 ($EO_{141}PO_{44}EO_{141}$) were obtained from Sigma–Aldrich Company Ltd. USA. The standard Pb(II) and other metal ions solutions were prepared from their corresponding AAS grade (1000 µg/mL) solutions and purchased from Wako Pure Chemicals, Osaka, Japan. For pH adjustments in detection operation, buffer solutions of 3–morpholinopropane sulfonic acid (MOPS) and 2–(cyclohexylamino)ethane sulfonic acid (CHES) were procured from Dojindo

Chemicals, Japan, and KCl, HCl, NaOH from Wako Pure Chemicals, Osaka, Japan. Ultra-pure water prepared with a Milli–Q Elix Advant 3 was used throughout this work.

2.2. Synthesis and characterization of the TSNT ligand

The preparation of major steps for the 1E,1`E,1``E,1```E (tetrakis(3-carboxysalicylidene)) naphthalene-1,2,5,5-tetramine (TSNT) are shown in **Scheme 1**. The TSNT was prepared by the reaction of naphthalene-1,2,5,6-tetraamine (0.25 moles) and 3-formyl-2-hydroxybenzoic acid (one mole) in ethanol and small amount of acetic acid was added. The resultant mixture was then heated under reflux for 4 hours and left to cool at room temperature. The solid formed upon cooling was collected by suction filtration. The separated product was recrystallized from the system dichloromethane/methanol 1/1 and the purpose product was dried at 50^{o}C for 24 h. The purity of the TSNT was analyzed by CHNS elemental analyses as follows: C, 64.59%; H, 3.56%; N, 7.15% as consistent with the $C_{42}H_{28}N_4O_{12}$ molecular formula, which requires C, 64.62%; H, 3.59%; N, 7.17%. The product was characterized by ^{1}H NMR spectroscopy. The ^{1}H NMR (400 MHz in $CDCl_3$) data of BSBAE are as follows: δ 5.35 (4H, Ph-OH), 7.29 (4H, p, Ph-OH), 8.0 (4H, o, Ph-OH), 8.01 (4H, naphthalene), 8.2 (4H, m, Ph-OH), 8.87 (4H, CH-imine), 11 (4H, carboxylic acid). ^{13}C NMR (400 MHz, $CDCl_3$): δ 113.4 (4C, Ph, Ph-COOH), 118.4 (4C, Ph, Ph-CH=N), 121.3 (4CH, Ph, p-Ph-OH), 133.4 (2C, naphthalene), 134.0 (4CH, Ph, o-Ph-OH), 144.1(4C, naphthalene), 160.0 (CH, imine), 162.6 (4C, Ph, Ph-OH), 171.8 (4C, carboxylic acid), where the Ph is the phenyl.

2.3. Preparation mesoporous silica and mesoporous adsorbent

The preparation of mesoporous silica monoliths procedure was involved by adding of TMOS and triblock copolymers (F108 ($EO_{141}PO_{44}EO_{141}$, MW: 14,600)) to obtain a homogenized sol–gel mixture based on the F108/TMOS mass ratio. The liquid crystal phase was achieved after quick addition of acidified aqueous solution and to promote hydrolysis of

the TMOS around the liquid crystal phase assembly of the triblock copolymer surfactants. However, the mesoporous silica monoliths were synthesized following the reported methods [**15,27**]. In typical conditions, the composition mass ratio of F108:TMOS:HCl/H_2O was 1.4:2:1 respectively. The homogeneous sol-gel synthesis was achieved by mixing F108/TMOS in a 200 mL beaker and then shaking at 60°C until homogeneous. The exothermic hydrolysis and condensation of TMOS occurred rapidly by addition of acidified aqueous solution of HCl (at pH = 1.3) to this homogeneous solution. The methanol produced from the TMOS hydrolysis was removed by a vacuum pump connected to a rotary evaporator at 45°C. Then the materials were dried at 45°C for 24 h to complete the drying process. The organic moieties were removed by calcination at 500°C for 6 h under the normal atmosphere. After calcinations, the material was ground properly and ready to use as substrates for fabrication adsorbent.

The mesoporous adsorbent was prepared by direct immobilization of TSNT (60 mg) in dimethylformamide (DMF) solution into 1.0 g mesoporous silica. The immobilization procedure was performed under vacuum at 50°C until TSNT saturation was achieved. The DMF was removed by a vacuum connected to a rotary evaporator at 80°C and the resulting mesoporous adsorbent was washed in warm water to check the stability and elution of TSNT from inorganic silica materials. Finally, the mesoporous adsorbent was dried at 45°C for 8 h and ground to fine powder for Pb(II) ions detection and removal experiments under optimum conditions. The TSNT immobilization amount (0.04 mmol/g) was calculated from the following equation:

$$Q = (C_i - C_f)\, V/m \quad (1)$$

where, Q is the adsorbed amount (mmol/g), V is the solution volume (L), *m* is the mass of mesoporous silica (g), C_i and C_f are the initial concentration and supernatant concentration of the TSNT, respectively.

2.4. Pb(II) ions detection, removal and reuses studies

In order to detect Pb(II), the mesoporous adsorbent was immersed in a mixture of specific Pb(II) ions concentrations (2.0 mg/L) and adjusted at appropriate pH of 2.01, 3.50 (0.2 M of KCl with 2.0 M HCl), 5.20 (0.2 M $CH_3COOHCH_3COONa$ with 1.0 M HCl), 7.01 (0.2 M MOPS with NaOH), 9.50 (0.2 M CHES with NaOH) at constant volume (10 mL) with shaking in a temperature-controlled water bath with a mechanical shaker at 25°C for 20 min at a constant agitation speed of 110 rpm to achieve good color separation. A blank solution was also prepared, following the same procedure for comparison with color formation. After color optimization, the solid materials were filtered using Whatman filter paper (25 mm; Shibata filter holder) and used for color assessment and absorbance measurements by solid-state UV–Vis–NIR spectrophotometer for the qualitative and quantitative Pb(II) ion estimation. The mesoporous adsorbent was ground to fine powder to achieve homogeneity in the absorbance spectra. The detection limit (L_D) of Pb(II) ions using the mesoporous adsorbent was determined from the linear part of the calibration plot according to the following equation [**28**]:

$$L_D = KS_b/m \quad (2)$$

where, K value is 3, S_b is the standard deviation for the blank and m the slope of the calibration graph in the linear range, respectively.

In removal operation, the mesoporous adsorbent was also immersed in Pb(II) ions concentrations and adjusted at specific pH values by adding of HCl or NaOH in 20 mL solutions and the amount of mesoporous adsorbent was 10 mg. After stirring for 1 h at room temperature, the solid materials were separated by filtration system and Pb(II) concentrations in before and after sorption operations were analyzed by ICP–AES. During the removal operation, the amount of adsorbed Pb(II) was calculated according to the following equations:

$$\text{Mass balance } q_e = (C_0 - C_f)\, V/M \text{ (mg/g)} \quad (3)$$

$$\text{and metal ion removal efficiency } Re = \frac{(C_0 - C_f)}{C_0} \times 100\ (\%) \quad (4)$$

where, V is the volume of the aqueous solution (L), and M is the weight of the mesoporous adsorbent (g), C_0 and C_f are the initial and final concentrations of Pb(II) ions in solutions, respectively.

To determine the kinetics performances, 10 mg of mesoporous adsorbent was added to 20 mL solution containing 5.0 mg/L concentrations of Pb(II) ions. The mixture was then stirred, and samples were filtered at different time intervals and the filtrate solution was analyzed by ICP–AES. In the case of maximum removal capacity, 10 mg of mesoporous adsorbent was also added in different concentration of Pb(II) ions and stirred (650 rpm) for 3 h and filtrate solutions were analyzed by ICP–AES.

In order to evaluate the reusability of the mesoporous adsorbent, elution experiments were conducted with pertinent concentration monoprotic acid. First, 20 mL of 5.0 mM Pb(II) ion solution was adsorbed by the 40 mg mesoporous adsorbent and then elution experiments were carried out using 0.20 M HCl acid. The adsorbed Pb(II) ions and adsorbent were washed with deionized water several times and transferred into 50 mL beaker. To this 5.0 mL of the eluting agent was added and the mixture was stirred for 15 min. The concentration of Pb(II) ions released from the adsorbent into aqueous phase was analyzed by ICP–AES. Then the mesoporous adsorbent was reused in several cycles and clarifies long-term use as cost-effective adsorbent. All experiments in this study were duplicated to assure the consistency and reproducibility of the results.

2.5. Analyses

The NMR spectra was obtained on a Varian NMR System 400MHz Wide-Bore Spectrometer. The N_2 adsorption-desorption isotherms were measured using the 3Flex analyzer (Micromeritics, USA) at 77 K.. Before the N_2 isothermal analysis, silica substrates were pre-treated at 100°C for 3 h under vacuum until the pressure was equilibrated to 10^{-3} Torr. The pore size distribution was measured from the adsorption isotherms curve by using

nonlocal density functional theory (NLDFT). The specific surface area (S_{BET}) was measured by using multi-point adsorption data from the linear segment of the N_2 adsorption isotherms using Brunauer–Emmett–Teller (BET) theory. Transmission electron microscopy (TEM) was obtained by using a JEOL (JEM-2100F) and operated at 200 kV. The TEM samples were prepared by dispersing the powder particles in ethanol solution using an ultrasonic bath and then dropped on copper grids. The absorbance spectrum of the adsorbent material was measured by UV–Vis–NIR spectrophotometer (Shimadzu, 3700) and metal ions concentrations were determined by ICP–AES (SII NanoTechnology Inc.). The ICP–AES instrument was calibrated using four standard solutions containing 0, 0.25, 0.5, 1.0 and 2.0 mg/L (for each element) and the correlation coefficient of the calibration curve was higher than 0.9999. In addition, sample solutions having complicated matrices were not used and no significant interference of matrices was observed.

3. Results and discussion

3.1. Mesoporous silica and mesoporous adsorbent

The large type-H_2 hysteresis loops and well-defined steepness of the N_2 isotherms indicate large with uniform cage structures mesoporous silica (**Fig. 1**) that was fabricated by using F108 as a soft template. The shift toward higher *P*/*P*o for the desorption isotherms indicates other enlarged pore entrances were connected without loss of cage periodicity in mesostructures. Therefore, the mesoporous silica has the appreciable textural parameters of specific surface area (S_{BET}), mesopore volume (Vp), and tunable pore diameters. The decrease in pore size, surface area, and pore volume correspond to the inclusion of TSNT ligand molecules into mesoporous carriers (**Fig. 1**(b)). In addition, the TSNT ligand has become rigid in inner pore surfaces and the retention of the physical characteristics of the mesoporous adsorbent could enhance the diffusion kinetics for Pb(II)-TSNT binding events, as evidenced

by the fast response time with the low-level Pb(II) detection and removal. Moreover, the tunable silica surfaces have significant advantages for direct immobilization of TSNT in which high loading capacity of TSNT was achieved with open specific activity of the TSNT functional groups.

The SEM images of as-synthesized samples prepared by an instant direct-templating method are shown in **Fig. 2(A,B).** A large cage with particle size of more than 200 μm has been fabricated due to the synthesis applying the emulsion as structure directing agent and the SEM pictures of the samples are typical for the silicate mesoporous materials and show large particle morphologies [**14,16**]. This synthesis method was believed to generate the bulk form of mesoporous silica cage monoliths. A higher magnification SEM image clarified the presence of macropores of various sizes ranging from 1 to 10 μm. The micrographs clearly revealed that the resulting particles were almost perfectly spherical in shape and size. The TEM images show (**Fig. 2(C,D)** highly ordered mesoporous structure, in which the pores were well arranged as mesocage structures, which indicated the direct interaction between TSNT ligand and silica into the rigid condensed pore surfaces with retention of the ordered structures, leading to high flux and efficient Pb(II) ion transport during the capturing system. The highly ordered porous structure of mesocage silica with average pore size is about 7.5 nm. In the preparation of the mesoporous adsorbent, the hydrogen bonding or hetero atoms bonding occurred between the abundant hydroxyl groups of pore surface silicates and the heteroatoms of the synthesized TSNT ligand molecule.

3.2. Pb(II) detection parameters

3.2.1. Effect of solution pH

In naked-eye Pb(II) detection, the effect of solution pH is depended on achieving the optimum color formation and sensitive detection. The optimum color formation and signaling response are possible based on the stable complexation and binding ability of Pb(II)–TSNT.

Therefore, a wide pH range from 2.0 to 9.5 using different buffer solutions in each pH region was investigated for Pb(II) ions detection and the absorbance spectra were carefully evaluated. The amount of mesoporous adsorbent dose was sufficient to achieve good color separation between the ‘‘blank’’ and Pb(II) ion–ligand ‘‘sample,’’ at ultra-trace Pb(II) ion concentration. The notable changes in color and absorbance intensity of the mesoporous adsorbent for Pb(II) was observed at pH 7.0 as shown in **Fig. 3**. The specific color intensity of $[Pb(II)–TSNT]^{n+}$ binding events on the mesoporous adsorbent at a specific pH region indicated the thermodynamic stability of the geometrical coordination.

3.2.2. Simple recognition and detection limit

The sensitive Pb(II)-spectral response of the mesoporous adsorbent ensured excellent optical Pb(II) isolations even at ultra-trace concentrations with significant color transitions as illustrated in **Fig. 4(A)**. The tunable mesoporous adsorbent showed phenomenal behavior in terms of sensitivity by forming stable chelate complexes with Pb(II) ions as $[Pb(II)–TSNT]^{n+}$. The quantification process for Pb(II) detection by the mesoporous adsorbent over μg/L to mg/L level concentrations was monitored via UV/Vis spectroscopy. Increasing in Pb(II) concentration from 0 to 2.0 mg/L, increases in the absorbance spectra correspond to color formation between mesoporous adsorbent and Pb(II) ions at pH 7.0. The absorbance spectra of the mesoporous adsorbent exhibited a shift from (λ_{max}) 375 nm to 350 nm, resulting from the binding of Pb(II) ions with the TSNT ligand (**Fig. 4(A)**). It is also noted that the shift from 510 nm to 455 nm was not consistent and the consistent shift was found from 375 nm to 350 nm with increasing the Pb(II) ions concentration based on the signal intensity measurement as judged from **Fig. 4(A)**. Therefore, the signaling responses indicated the formation of charge-transfer $[Pb(II)–TSNT]^{n+}$ complexes and stable complexation at pH 7.0. The naked-eye observation of rapid and sensitive detection of Pb(II) at ultra-trace concentrations by using such a mesoporous adsorbent indicated the high performance and reliability of this detection

system. The mesoporous adsorbent led to simple separation and visual detection over a wide range of concentrations, as well as the sensitive quantification of analyte ions at trace levels. The results also evidence that the color change provided a simple procedure for sensitive Pb(II) detection without using of sophisticated instruments [**15,27]**.

Fig. 4(B) shows the calibration plot of the TSNT-modified mesoporous adsorbent during Pb(II) detection. The quantification measurements were performed using a wide range of concentrations (up to 2.0 mg/L) from Pb(II) ions under optimum detection conditions. The linear correlation at low concentration ranges indicated that the Pb(II) ions can be detected with high sensitivity over a wide range of concentrations (0.024 to 0.483 µM). Moreover, a nonlinear correlation at the inflection point was evident to the highest Pb(II) ion concentration (over 0.483 µM), indicating that mesoporous adsorbent is efficient at low-level concentrations of Pb(II) ions. The standard deviation of the Pb(II) ion analysis was 1.5% as evidenced by the fitting plot of the calibration (**Fig. 4(B)**, inset). The capability of the detection assays is highly sensitive to detect ultra-trace Pb(II) ions. The limit of detection (L_D) of Pb(II) ions using the mesoporous adsorbent was 0.11 µg/L. This finding indicates that the tunable mesoporous adsorbent can effectively separate the Pb(II) ions at trace concentrations.

3.2.3. Ion selectivity of the mesoporous adsorbent

The specific ions selectivity is a key consideration in Pb(II) detection by ligand immobilized tunable mesoporous adsorbent. Therefore, the proposed mesoporous adsorbent was evaluated under optimum conditions using other environmental relevant metal ions such as Co(II), Cd(II), Cu(II), Mn(II), Zn(II), Na(I), Fe(II), Al(III), Hg(II) and Fe(III). For comparison, the concentrations of Pb(II) (2.0 mg/L) and other metal ions are kept identical (30 mg/L), and the changes in the absorbance with the addition of each metal ion were evaluated. **Fig. 5** shows the color profiles and absorbance spectra of the blank sample and after the addition of cations and anions. Experimental results indicated that added metal ions with

concentrations up to 2.0 mg/L could not induce the significant changes in the absorbance spectra of mesoporous adsorbent except Pb(II) ions. This is due to the orientation and arrangement of the TSNT assemblies mounted onto mesoporous silica with open-pore arrays and high surface areas which allowed stable thermodynamic binding of $[Pb(II)\text{-}TSNT]^{n+}$. However, with the addition of high doses of these actively interfered metal ions to Pb(II) ions detection system, a high disturbance (±10%) in the quantitative Pb(II) ions detection data was summarized in **Table 1.** Despite the minimal increase in the reflectance spectra of the adsorbent, with the addition of Co(II) and Cu(II) as disturbance species there were slight changes in both the color map and signal intensity when its concentrations in solution exceeded 20 mg/L. However, after addition of masking agent (0.10 M sodium thiosulfate), Co(II) and Cu(II) interferences were eliminated in Pb(II) ions detection system [**11**]. The results clarified that mesoporous adsorbent is highly selective to Pb(II) ions even in the presence of numerous environmentally relevant metal ions.

3.3. Pb(II) ions removal parameters

3.3.1. Effect of pH

The pH of the aqueous solution is the most critical parameter for metal sorption as it influences both the mesoporous surface chemistry as well as the solution chemistry of soluble metal ions. Therefore, the effect of pH on Pb(II) sorption onto the mesoporous adsorbent, the batch sorption equilibrium was studied at different pHs in the range of 2.0–9.5. The Pb(II) removal onto the mesoporous adsorbent was pH dependent as shown in **Fig. 6(A)**. The results clarified that Pb(II) removal by the mesoporous adsorbent was very low in the acidic pH region, but increased rapidly with increasing pH and then reached the maximum at pH 7.0. The lower Pb(II) removal at low solution pH values may be attributed to the competitive sorption effect of the H^+ ions. One of the reasons for metal ions sorption is that the inert organic matter mesoporous surface contains a large number of active sites [**14,15**]. The Pb(II) removal

depends on the nature of the active sites of mesoporous adsorbent and of the Pb(II) ions in solution. Therefore the maximum removal efficiency depends on the type of inert organic matter as well as on the type of metal ions for a given inert organic matter at the specific pH region. The other experimental parameters for Pb(II) removal parameters were carried out at pH 7.0 region in this study.

3.3.2. Effect of contact time

The time-dependent behavior of Pb(II) removal was measured by varying the equilibrium time between the adsorbate and mesoporous adsorbent in the range of 10–80 min. The Pb(II) concentration was kept as 5.0 mg/L while the amount of mesoporous adsorbent was 10 mg. The removal efficiency is shown in **Fig. 6(B)** as a function of contact time. The data confirmed that the Pb(II) removal versus time curve was single, smooth and continuous leading to saturation, suggesting the possible monolayer coverage of Pb(II) ions on the surface of the mesoporous adsorbent. The mesoporous adsorbent shows a sorption increase with increasing time and exhibited a rapid removal during the short contact time, followed by a slow increase until equilibrium was reached. This two steps removal was previously reported by several adsorbents [**3,8,18**]. The rapid step is quantitatively predominant and probably due to the abundant availability of active sites on the mesoporous adsorbent surface. The second step is slow and quantitatively insignificant with gradual occupancy of the pore surface active functional sites. The fast removal could be attributed to the external and internal surface adsorption. The data also indicated that the equilibrium between the Pb(II) and mesoporous adsorbent was attained within 40 min. Then a shaking time of 3 h was assumed to be suitable for subsequent removal experiments in this work for measuring the maximum sorption capacity by the mesoporous adsorbent.

3.3.4. Effect of competing ions in Pb(II) removal

There are several cations co-existing such as K(I), Ag(I), Na(I), Ni(II), Ca(II), Zn(II), Ba(II), Co(II), Mg(II), Cd(II), Cu(II), Mn(II), Fe(II), Cr(III), Al(III), Hg(II) and Fe(III) in water with Pb(II) ions. Therefore the selectivity approach for Pb(II) ions was evaluated by investigating the metal removal efficiency for the system to ten other common metal ions including K(I), Na(I), Ag(I), Ca(II), Zn(II) Ni(II), Hg(II), Ba(II), Mg(II), and Cr(III) ions. The initial solution was prepared with 10 mg/L in each of above mentioned ten metal ions in one beaker (50 mL) and Pb(II) ions in 1.0 mg/L in a 20 mL solution at pH 7.0. Then 10 mg of mesoporous adsorbent was added and stirred for 1 h. After filtration, the filtrate solution was checked by ICP–AES. The Pb(II) ion was adsorbed via changing the color. A significant selectivity for Pb(II) ions was observed at a 10-fold excess of other metal ions as shown in **Fig. 7**. The data also suggested that the proposed mesoporous adsorbent could be applied for the sensitive analysis and removal of low-level Pb(II) in environmental matrices.

3.3.3. Sorption isotherms

The sorption isotherm is described by the sorption equilibrium in the degree of interaction between the amounts of adsorbate on the adsorbents. However, the Langmuir sorption isotherm describes the relationship between the amount adsorbed by a unit adsorbent weight and the amount of solute remaining in the solution at equilibrium assuming that the presences of a finite number of binding sites are homogeneously distributed over the adsorbent surface and presenting the same affinity for sorption of monolayer coverage. Then the Langmuir equation has been successfully applied to this sorption operation as follows:

$$C_e/q_e = 1/(K_L q_m) + (1/q_m)C_e \quad \text{(linear form)} \qquad (5)$$

where, q_m is the maximum sorption capacity, K_L is the Langmuir sorption equilibrium constant; C_e and q_e are the concentration of the adsorbate in the equilibrated solution and the amount of

adsorbed on mesoporous adsorbent, respectively. The q_m and K_L are the Langmuir constants which are related to the sorption capacity and energy of sorption, respectively, and can be calculated from the intercept and slope of the linear plot, with C_e/q_e versus C_e as shown in **Fig. 8(A)** (inset). However, the linear fits to experimental data were obtained by the Langmuir isotherms equation. The linear plot of C_e/q_e versus C_e shows that the sorption obeys the Langmuir model by mesoporous adsorbent. The maximum sorption capacity is corresponding to complete single layer and showed a mass capacity of 184.32 mg/g. The high sorption capacity obtained by mesoporous adsorbent because mesoporous adsorbent has spherical nanosized cavities leading to high flux and Pb(II) ion uptake. The essential characteristics in the Langmuir isotherm model are embodied in a separation factor which is dimensionless equilibrium parameter R_L described as follows:

$$R_L = 1/ (1 + K_L C_0) \quad (6)$$

where, C_0 (mg/L) is the highest initial ions concentration. Accordingly, observing R_L value to be positive and lying between 0 and 1. The R_L value is less than 1, confirm the favorability of the sorption isotherm. The main criterion of the nature of an isotherm involved is as follows: $R > 1$, unfavorable; R=1, linear; $0 < R < 1$, favorable and $R = 0$, irreversible isotherm. The R_L value for Pb(II) of mesoporous adsorbent was 0.061 indicating the sorption process was favorable. The obtained sorption capacities of the adsorbents are comparable to other adsorbents from the literature and are given in **Table 2**. The comparison data shows that the mesoporous adsorbent outperforms significantly many other sorbents and was verified as promising for the Pb(II) removal from contaminated water streams.

3.3.5. Elution and reuses studies

The elution and regeneration of the mesoporous adsorbent are likely to be a key factor in improving process economics and cost effective materials. To evaluate an exact eluent for regeneration and reusability of mesoporous adsorbent, we performed the elution experiments

using different eluents. However, Pb(II) elution from the Pb(II)-mesoporous adsorbent beads was also performed in a batch experimental approach. The reusability was checked by following the sorption–elution–regeneration processes for eight cycles and sorption efficiency in each cycle was measured. Various factors are involved in determining Pb(II) elution rates to the extent of hydration of Pb(II) ions and microstructure cage cavities of the mesoporous adsorbent. However, using HCl as an eluent, the coordination spheres of complexed Pb(II) ions is disrupted and subsequently Pb(II) ions are released from the mesoporous adsorbent surface into the elution medium. In this study, 20 mg of mesoporous adsorbent was mixed in 30 mL of 200 mg/L Pb(II) for sorption operation and 5 mL of 0.30 M HCl was used as an eluent. The elution time was found to be 10 min. The possible complexation bonding mechanism and elution of Pb(II) is shown in **Scheme 2**. **Fig. 8(B)** shows the relationship between the time for reuses and the sorption capacity of the mesoporous adsorbent for Pb(II) ions. It can be seen that the sorption capacity of the mesoporous adsorbent decreased slightly after eight cycles. The mesoporous adsorbent exhibited high meso–structural stability, active functional sites, and high surface area with large pore volume which imply the potential for several reuses of the adsorbent. This means that the newly fine-tuned mesoporous adsorbent has a great potential for industrial Pb(II) removal applications.

4. Conclusions

To detect and remove low level toxic metal at the nanoscale level will lead to new frontiers in nanotechnology and materials science, and tunable and sensitive materials are essential. Therefore the mesostructured designed mesoporous adsorbent in this study exhibited interesting selective behavior that permits accurate, specific detection and removal of Pb(II) ions with high efficiency. The design of tunable mesoporous adsorbent was prepared based on 1E,1`E,1``E,1```E (tetrakis(3-carboxysalicylidene))naphthalene-1,2,5,5-tetramine (TSNT)

ligand onto mesoporous silica monoliths by the direct immobilization method. A batch detection and removal study has been reported on the sorption of water soluble Pb(II) on mesoporous adsorbent. The newly prepared mesoporous adsorbent enabled the detection and removal responses according to Pb(II)–TSNT binding events by stable complexation mechanism based on charge transfer ((intense π–π transition) transduction. The presence of coexisting ions did not affect Pb(II) ions detection and sorption systems and mesoporous adsorbent efficiently removed the Pb(II) ion from multi ion mixture solutions. The Langmuir isotherm was satisfactorily employed to explain Pb(II) sorption at pH 7.0. The detection limit and maximum sorption capacity of the mesoporous adsorbent for Pb(II) at optimum conditions were 0.11 µg/L and 184.32 mg/g, respectively. The reducibility and reversibility of the chemical mesoporous adsorbent remains a unique and interesting challenge, as the mesostructured adsorbent can extend the control of Pb(II) ions detection and removal even after several regeneration cycles of the elution process. The reversibility, reusability with adsorption capacity and stability of the mesoporous adsorbent implied the high cost-effectiveness for Pb(II) removal from water. The present work showed the potential of mesoporous adsorbent to remove heavy metal ions as well as to separate one from another for possible removal in wastewater purification.

Acknowledgments

This research was partially supported by the Grant-in-Aid for Research Activity Start-up (24860070) from the Japan Society for the Promotion of Science. The authors also wish to thank the anonymous reviewers and editor for their helpful suggestions, remarks and enlightening comments. Christopher Paul Taylor is greatly acknowledged for his valuable support in English language editing.

References

[1] J.O. Nriagu, J.M. Pacyna, Quantitative assessment of worldwide contamination of air, water and soils by trace metals, Nature 333 (1988) 134–139.

[2] N. Gupta, S.S. Amritphale, N. Chandra, Removal of lead from aqueous solution by hybrid precursor prepared by rice hull, Journal of Hazardous Materials 163 (2009) 1194–1198.

[3] Y.X. Liu, J.M. Yan, D.X. Yuan, Q.L. Li, X.Y. Wu, The study of lead removal from aqueous solution using an electrochemical method with a stainless steel net electrode coated with single wall carbon nanotubes, Chemical Engineering Journal 218 (2013) 81–88.

[4] P.M. Pimentel, G. Gonzalez, M.F.A. Melo, D.M.A. Melo, C.N. Silva Jr., A.L.C. Assuncao, Removal of lead ions from aqueous solution by retorted shale, Separation and Purification Technology 56 (2007) 348–353.

[5] ATSDR, CERCLA Priority List of Hazardous Substances, 2007 (cited; available from: http://www.atsdr.cdc.gov/cercla/07list.html).

[6] E.M. Ali, Y. Zheng, H. Yu, J.Y. Ying, Ultrasensitive Pb^{2+} detection by glutathione capped quantum dots, Analytical Chemistry 79 (2007) 9452–9458.

[7] M. Tsunekawa, M. Ito, Y. Sasaki, T. Sakai, N. Hiroyoshi, Removal of lead compounds from polyvinylchloride in electric wires and cables using cation-exchange resin, Journal of Hazardous Materials 191 (2011) 388–392.

[8] V.K. Gupta, S. Agarwal, T.A. Saleh, Synthesis and characterization of alumina-coated carbon nanotubes and their application for lead removal, Journal of Hazardous Materials 185 (2011) 17–23.

[9] United States Environmental Protection Agency (USEPA), Drinking water contaminants, http://water.epa.gov/drink/contaminants/index.cfm#List.

[10] J. Richardson, A. Drake, C. Lazo-Miller, J. Hand, T. Morgan, I. Lagadic, Lead detection in environmental water sample using an organoclay film-based attenuated total reflectance sensor, Sensors Actuators B: Chemical 158 (2011) 271– 277.

[11] Q. Zhao, X. Rong, H. Ma, G. Tao, Dithizone functionalized CdSe/CdS quantum dots as turn-on fluorescent probe for ultrasensitive detection of lead ion, Journal of Hazardous Materials 250– 251 (2013) 45–52.

[12] J.Y. Kwon, Y.J. Jang, Y.J. Lee, K.M. Kim, M.S. Seo, W. Nam, J. Yoon, A highly selective fluorescent chemosensor for Pb^{2+}, Journal of the American Chemical Society 127 (2005) 10107–10111.

[13] N. Ding, H. Zhao, W. Peng, Y. He, Y. Zhou, L. Yuan, Y. Zhang, A simple colorimetric sensor based on anti-aggregation of gold nanoparticles for Hg^{2+} detection, Colloid and Surfaces A: Physicochemical Engineering Aspects 395 (2012) 161–167.

[14] (a) M.R. Awual, T. Yaita, Rapid sensing and recovery of palladium(II) using N,N-bis(salicylidene)1,2-bis(2-aminophenylthio)ethane modified sensor ensemble adsorbent, Sensors Actuators B: Chemical 183 (2013) 332–341; (b) M.R. Awual, M.A. Khaleque, Y. Ratna, H. Znad, Simultaneous ultra-trace palladium(II) detection and recovery from wastewater using new class meso-adsorbent, Journal of Industrial and Engineering Chemistry, (2014) http://dx.doi.org/10.1016/j.jiec.2014.02.053.

[15] (a) M.R. Awual, T. Yaita, H. Shiwaku, Design a novel optical adsorbent for simultaneous ultra-trace cerium(III) detection, sorption and recovery, Chemical Engineering Journal 228 (2013) 327–335; (b) M.R. Awual, M.M. Hasan, Fine-tuning mesoporous adsorbent for simultaneous ultra-trace palladium(II) detection, separation and recovery, Journal of Industrial and Engineering Chemistry, (2014) http://dx.doi.org/10.1016/j.jiec.2014.03.013.

[16] (a) M.R. Awual, M. Ismael, Efficient gold(III) detection, separation and recovery from urban mining waste using a facial conjugate adsorbent, Sensors and Actuators B:

Chemical, 196 (2014) 457–466; (b) M.R. Awual, T. Kobayashi, Y. Miyazaki, R. Motokawa, H. Shiwaku, S. Suzuki, Y. Okamoto, T. Yaita, Evaluation of lanthanide sorption and their coordination mechanism by EXAFS measurement using novel hybrid adsorbent, Chemical Engineering Journal 225 (2013) 558–566.

[17] Y. Deng, Z. Gao, B. Liu, X. Hu, Z. Wei, C. Sun, Selective removal of lead from aqueous solutions by ethylenediamine modified attapulgite, Chemical Engineering Journal 223 (2013) 91–98.

[18] S. Zhang, F. Xu, Y. Wang, W. Zhang, X. Peng, F. Pepe, Silica modified calcium alginate–xanthan gum hybrid bead composites for the removal and recovery of Pb(II) from aqueous solution, Chemical Engineering Journal 234 (2013) 33–42.

[19] M.A.M. Khraisheh, Y.S. Al-degs, W.A.M. Mcminn, Remediation of wastewater containing heavy metals using raw and modified diatomite, Chemical Engineering Journal 99 (2004) 177–184.

[20] M. Al-Harahsheh, R. Shawabkeh, A. Al-Harahsheh, K. Tarawneh, M.M. Batiha, Surface modification and characterization of Jordanian kaolinite: Application for lead removal from aqueous solutions, Applied Surface Science 255 (2009) 8098–8103.

[21] M. Kragovic, A. Dakovic, M. Markovic, J. Krstic. G.D. Gatta, N. Rotiroti, Characterization of lead sorption by the natural and Fe(III)-modified zeolite, Applied Surface Science 283 (2013) 764– 774.

[22] M. Martin-Lara, G. Blazquez, A. Ronda, I. Rodriguez, M. Calero, Multiple biosorption–desorption cycles in a fixed-bed column for Pb(II) removal by acid-treated olive stone, Journal of Industrial and Engineering Chemistry 18 (2012) 1006–1012.

[23] M.A. Salam, G. Al-Zhrani, S.A. Kosa, Simultaneous removal of copper(II), lead(II), zinc(II) and cadmium(II) from aqueous solutions by multi-walled carbon nanotubes, C. R. Chimie 15 (2012) 398–408.

583 [24] J. Huang, M. Ye, Y. Qu, L. Chu, R. Chen, Q. He, D. Xu, Pb (II) removal from aqueous
584 media by EDTA-modified mesoporous silica SBA-15, Journal of Colloid & Interface
585 Science 385 (2012) 137–146.
586 [25] H.T. Fan, J.B. Wu, X.L. Fan, D.S. Zhang, Z.J. Su, F. Yan, T. Sun, Removal of
587 cadmium(II) and lead(II) from aqueous solution using sulfur-functionalized silica
588 prepared by hydrothermal-assisted grafting method, Chemical Engineering Journal 198–
589 199 (2012) 355–363.
590 [26] H.M. Al-bishri, T.M. Abdel-Fattah, M.E. Mahmoud, Immobilization of [Bmim+Tf_2N^-]
591 hydrophobic ionic liquid on nano-silica-amine sorbent for implementation in solid phase
592 extraction and removal of lead, Journal of Industrial and Engineering Chemistry 18
593 (2012) 1252–1257.
594 [27] (a) M.R. Awual, M. Ismael, T. Yaita, S.A. El-Safty, H. Shiwaku, Y. Okamoto, S. Suzuki,
595 Trace copper(II) ions detection and removal from water using novel ligand modified
596 composite adsorbent, Chemical Engineering Journal 222 (2013) 67–76; (b) M.R.
597 Awual, I.M.M. Rahman, T. Yaita, M.A. Khaleque, M. Ferdows, pH dependent Cu(II)
598 and Pd(II) ions detection and removal from aqueous media by an efficient mesoporous
599 adsorbent, Chemical Engineering Journal, 236 (2014) 100–109.
600 [28] (a) M.R. Awual, T. Yaita, S.A. El-Safty, H. Shiwaku, S. Suzuki, Y. Okamoto, Copper(II)
601 ions capturing from water using ligand modified a new type mesoporous adsorbent,
602 Chemical Engineering Journal 221 (2013) 322–330; (b) M.R. Awual, M. Ismael, T.
603 Yaita, Efficient detection and extraction of cobalt(II) from lithium ion batteries and
604 wastewater by novel composite adsorbent, Sensors Actuators B: Chemical 191 (2014) 9–
605 18.
606
607
608

Table 1

Tolerance limit for interfering ions during detection of 2.0 mg/L Pb(II) ions by using mesoporous adsorbent

Tolerance limit for cations (mg/L) in solution												
K^+	Ag^+	Cu^{2+}	Ca^{2+}	Zn^{2+}	Ba^{2+}	Ni^{2+}	Mg^{2+}	Fe^{3+}	Ni^{2+}	Hg^{2+}	Co^{2+}	Al^{3+}
60	40	45[a]	110	50	45	50	60	100	45	35	40 [a]	75
Tolerance limit for anions (mg/L) in solution												
Cl^-	NO_3^-	HCO_3^-	CO_3^{2-}	SO_3^{2-}	SO_4^{2-}	PO_4^{3-}	SCN^-	ClO_4^-				
1200	850	700	600	500	650	550	675	675				

[a] suppressing agent of 0.1 M sodium thiosulfate

Table 2

Comparison of maximum sorption capacities of Pb(II) with different adsorbent materials.

Used materials	Maximum sorption capacity (mg/g)	Ref.
Attapulgite	258.0	[17]
Hybrid bead composites	25.84	[18]
Commercial activated carbon (F-400)	22.00	[19]
Diatomite	24.90	[19]
Jordanian kaolinite	54.35	[20]
Fe(III)-modified zeolite	98.72	[21]
EDTA-modified mesoporous silica	273.2	[24]
Sulfur-functionalized silica	46.30	[25]
Nano-silica-amine sorbent	269.1	[26]
Mesoporous adsorbent	184.32	This study

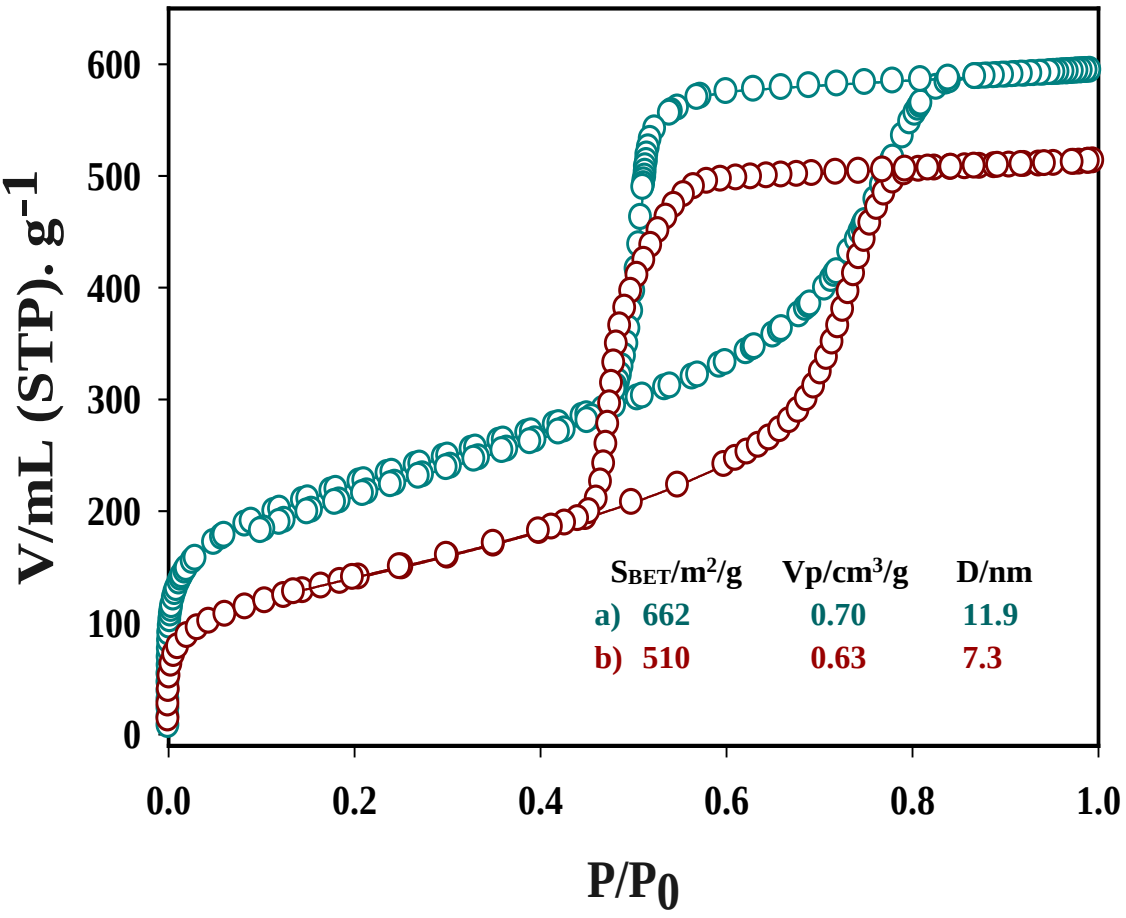

Fig. 1. N_2 adsorption and desorption isotherms of (a) inorganic mesoporous silica and (b) mesoporous adsorbent with different surface areas, pore sizes and pore volumes.

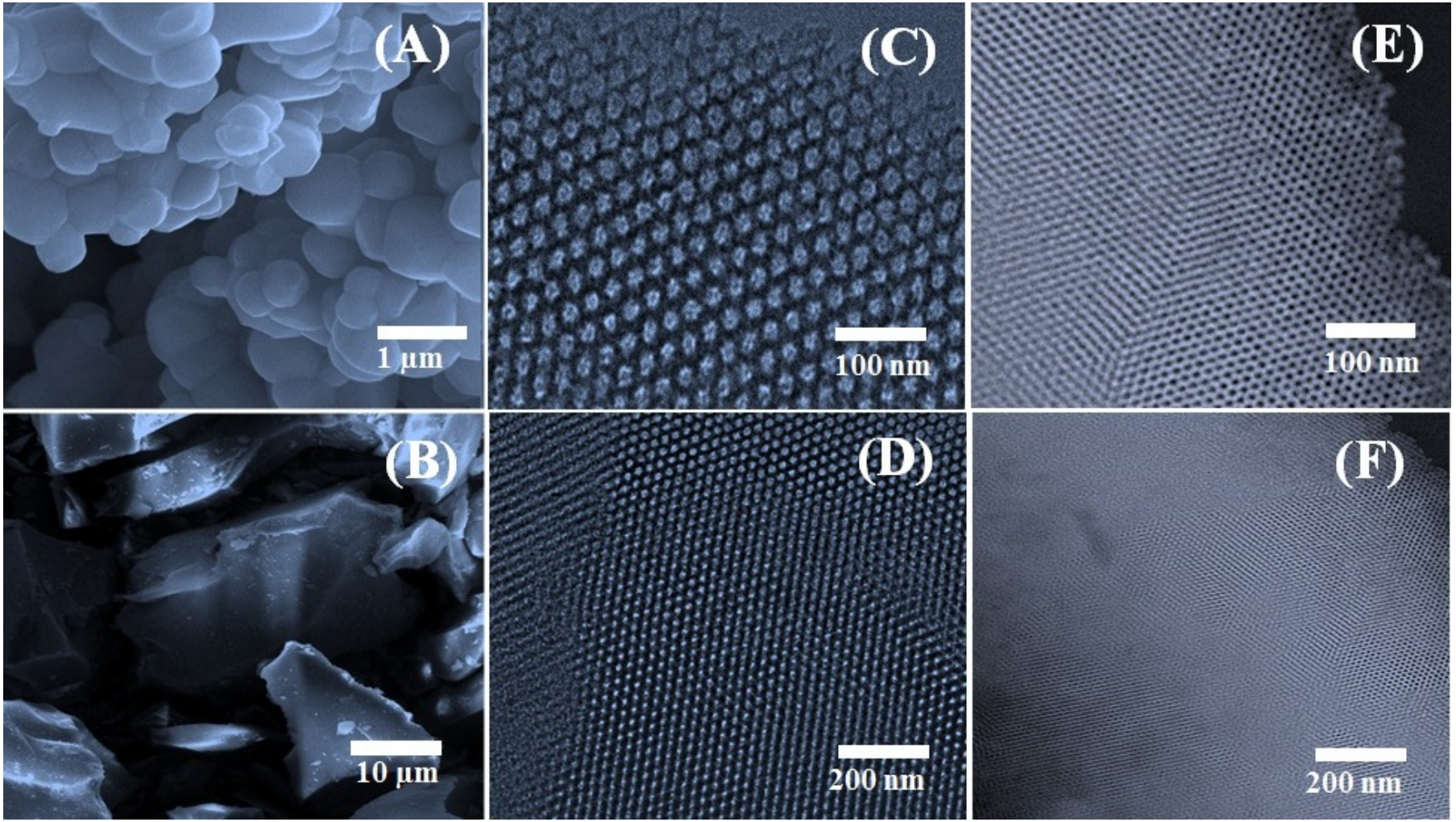

Fig. 2. SEM images of mesoporous silica monoliths fabricated by using an instant direct-templating method of lyotropic liquid crystalline phase (A) and (B); TEM images representative of ordered structures along with uniformly arranged mesopores (C, D) and STEM images of TSNT immobilized mesoporous adsorbent (E, F).

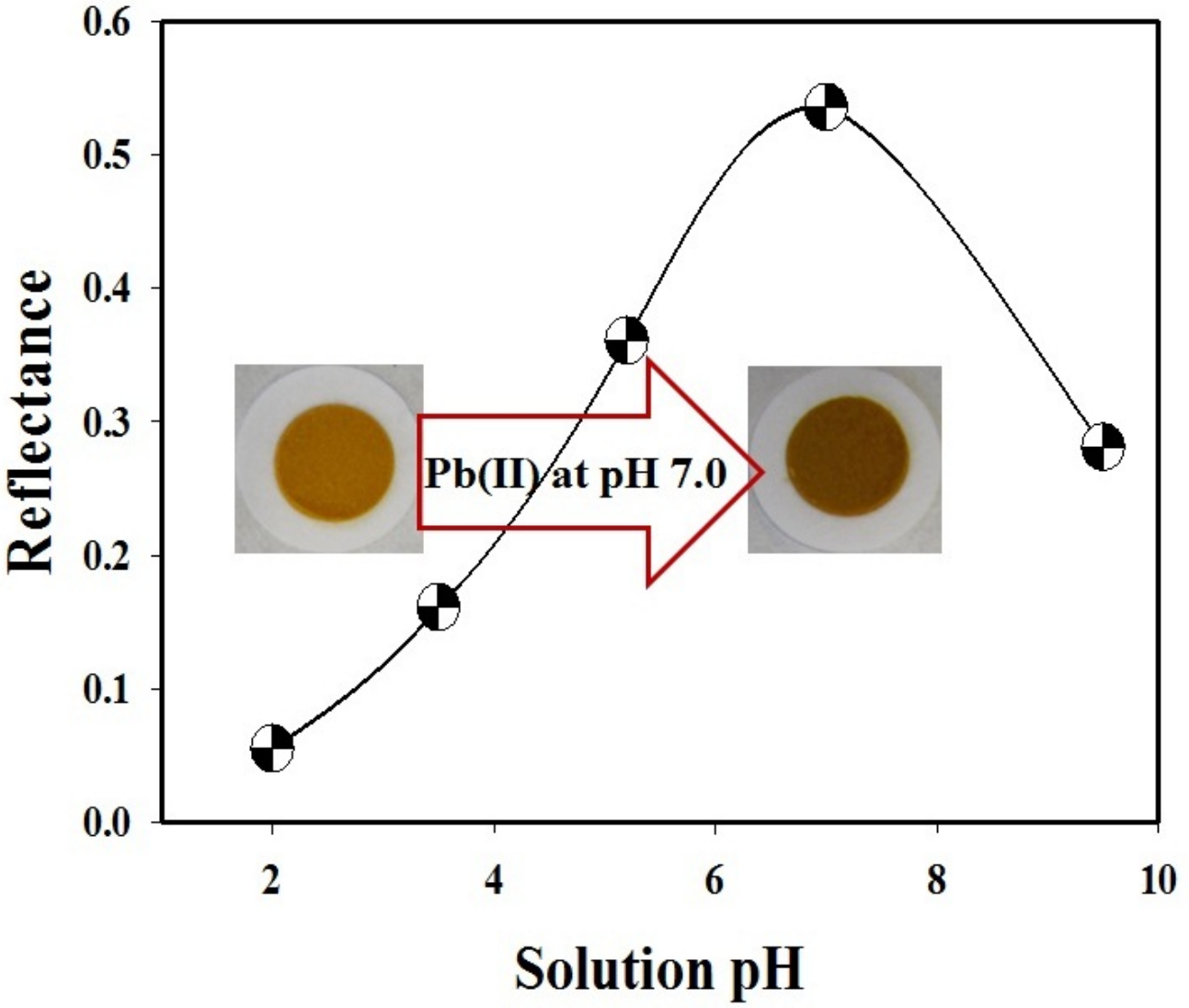

Fig. 3. Influence of solution pH for optical detection of Pb(II) ion by tunable mesoporous adsorbent when equilibrated individually at different pH conditions with 2.0 mg/L of Pb(II) ions at 25 °C in 10 mL volume for 20 min. The standard deviation was >3.0% for the analytical data of duplicate analyses.

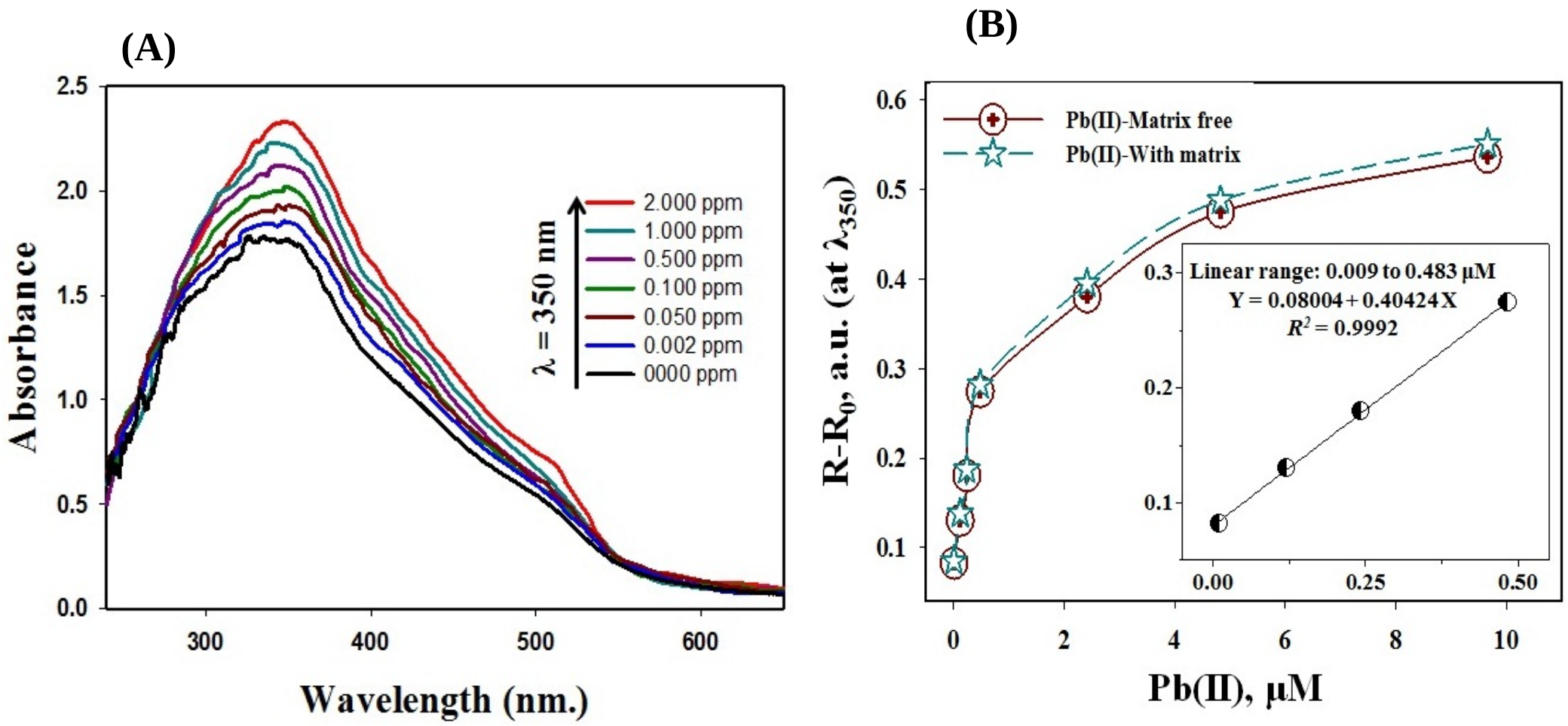

Fig. 4. (A) Color transition profiles and absorbance spectra observed with increasing concentrations of Pb(II) ions at pH 7.0; (B) Calibration curve with spectral absorbance measured at 350 with Pb(II) ion concentrations. The insets in the graph (B) show the low-limit colorimetric responses of Pb(II) ions with a linear fit line in the linear concentration range before saturating the calibration curve. The dotted line represents the calibration plot of the Pb(II) ions in the presence of active interfering species (listed in Fig. 5; concentration was the same in each points as that of Pb(II) ions) under the same sensing conditions. The error bars denote a relative standard deviation of ≥1.5% range for the analytical data of three replicated analyses.

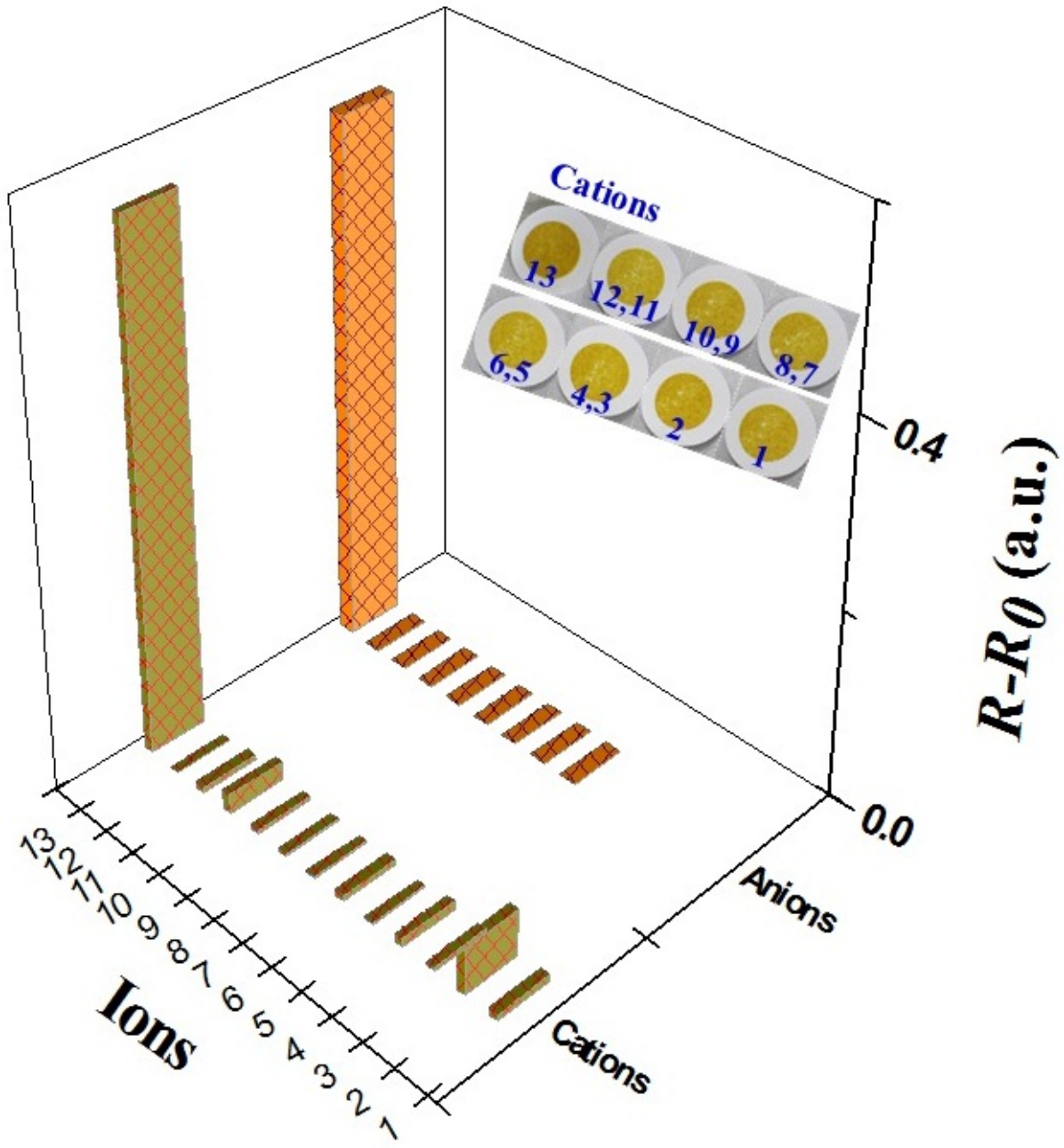

Fig. 5. Ion selective profiles of (2.0 mg/L) Pb(II) ions by the mesoporous adsorbent after adding various competing ions at optimal capture conditions (pH 2.0; 10 mg of mesoporous adsorbent and 20 mL volume). The interfering cations (30.0 mg/L) are listed in order (1 to 12): (1) K^{+} (2) Cu^{2+}, (3) Cd^{2+}, (4) Na^{+}, (5) Mn^{2+}, (6) Zn^{2+}, (7) Al^{3+}, (8) (9) Fe^{3+}, (10), Co^{2+}, (11) Hg^{2+}, (12) Blank and (13) 2.0 mg/L Pb^{2+}. The interfering (100 mg/L) anions are listed in order (5 to 12): (5) chloride, (6) nitrate, (7) sulfite, (8) sulfate, (9) bicarbonate, (10) carbonate, (11) phosphate and (12) perchlorate.

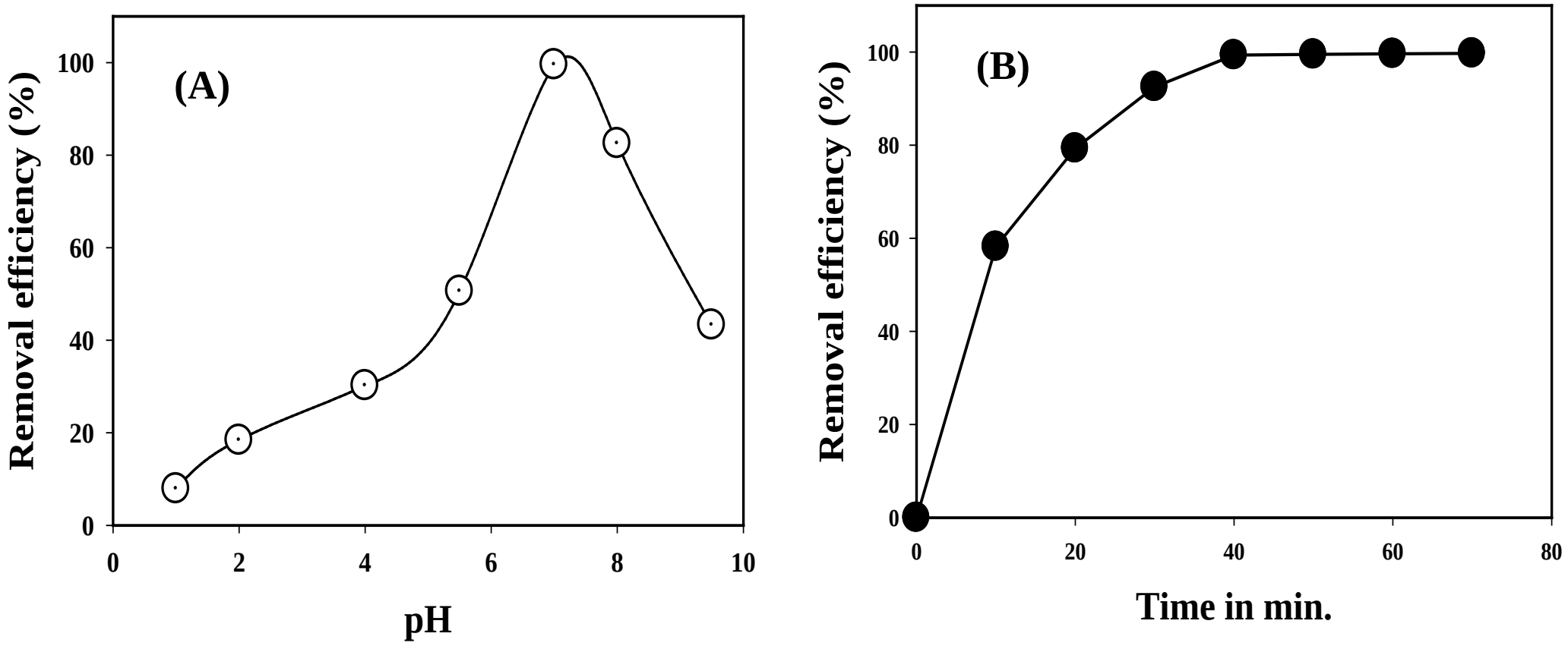

Fig. 6. Influence of (A) maximum Pb(II) ions removal under different pH regions; (B) equilibrium contact time for maximum Pb(II) ions removal when Pb(II) concentration was 5.0 mg/ in 20 mL. The RSD value was ~4.0%.

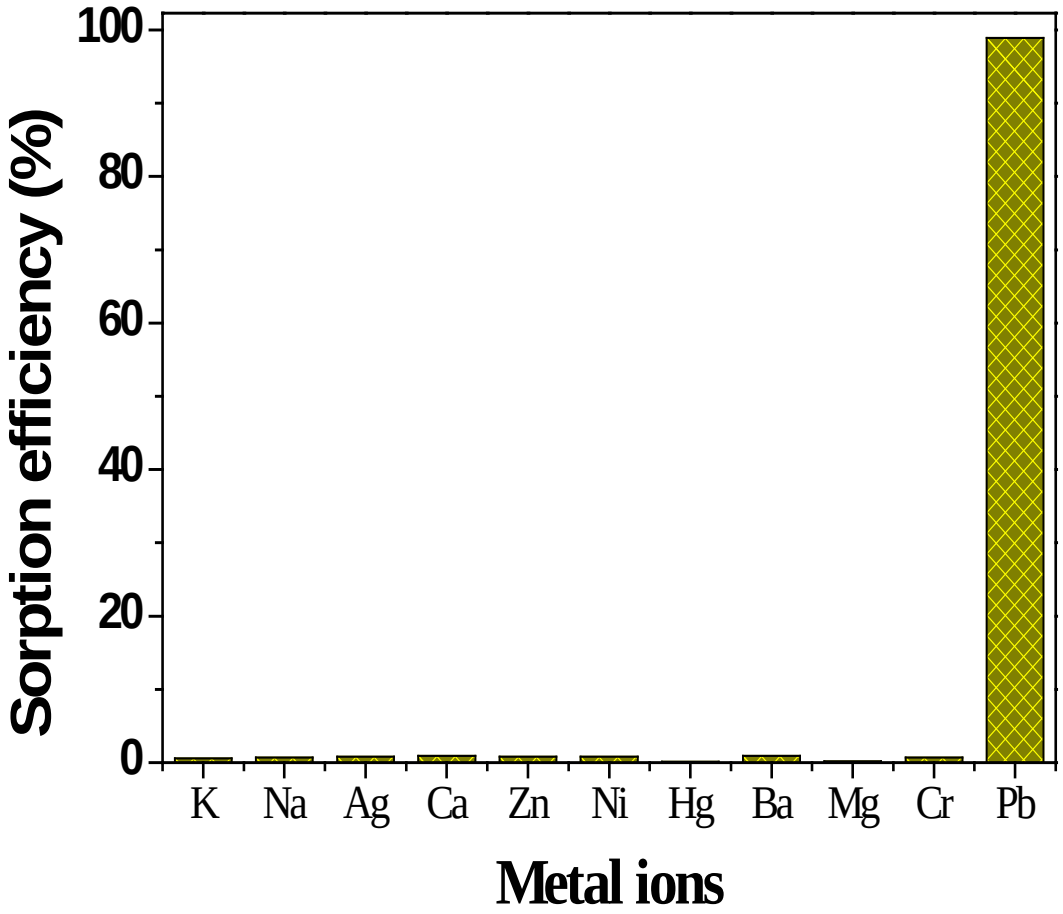

Fig. 7. Effect of competing ions in Pb(II) removal when Pb(II) and other metal ions concentration were 1.0 mg/L and 10.0 mg/L in each, respectively. The RSD value was ~3.5%.

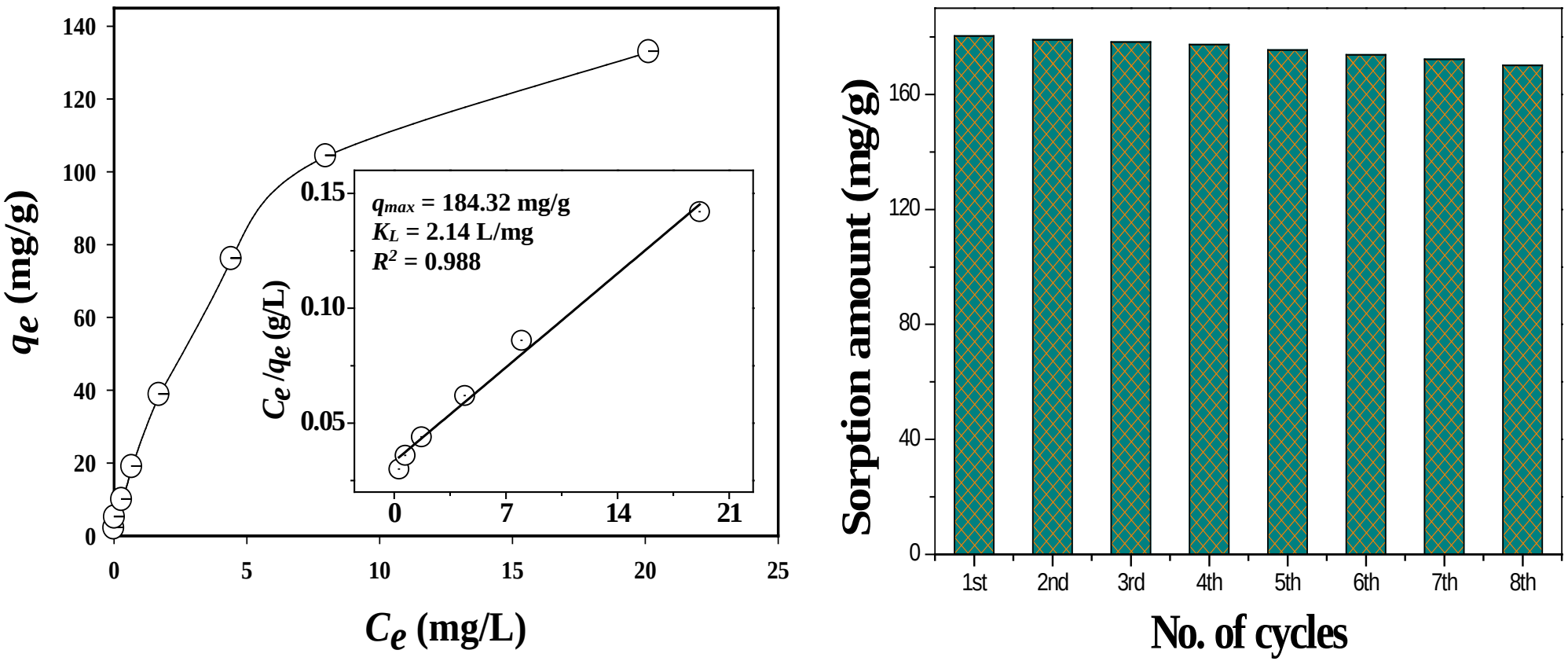

Fig. 8. (A) Langmuir sorption isotherms for Pb(II) ions sorption by mesoporous adsorbent and the linear (inset) form of the Langmuir plot (initial Pb(II) ion concentration range 0.50 – 80 mg/L; solution pH 7.0; adsorbent dose 10 mg; contact time 3 h); (B) Reusability performances of the mesoporous adsorbent after elution of Pb(II) and reuses in a number of cycles. The RSD value was ~4.5%.

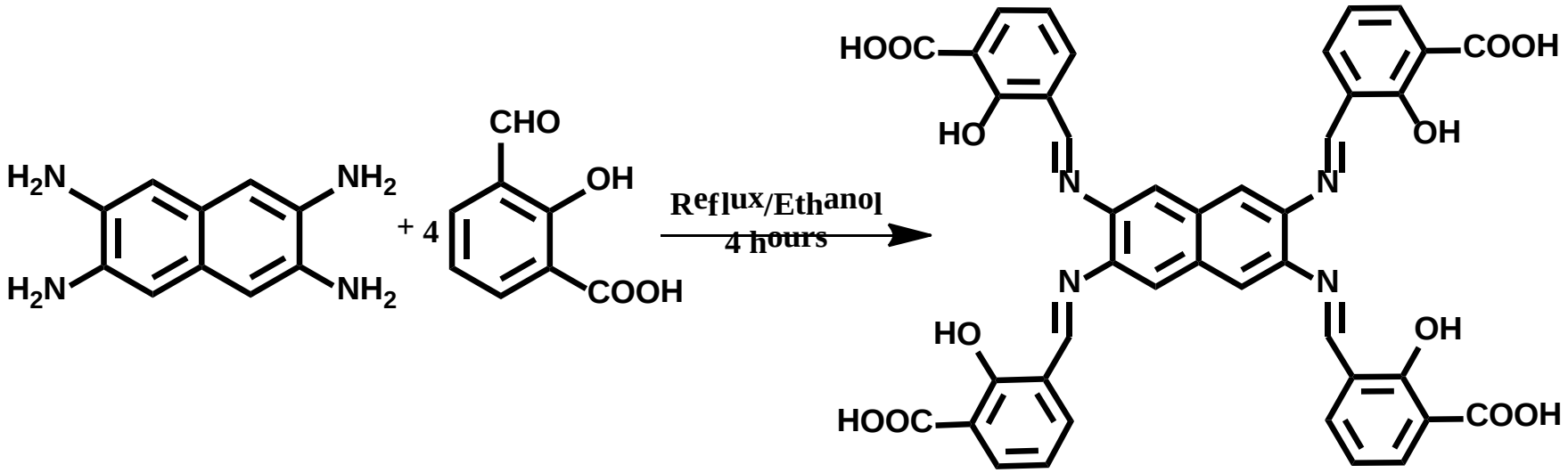

Scheme 1. Synthetic route for the preparation of 1E,1`E,1``E,1```E (tetrakis(3-carboxysalicylidene))naphthalene-1,2,5,5-tetramine (TSNT) ligand.

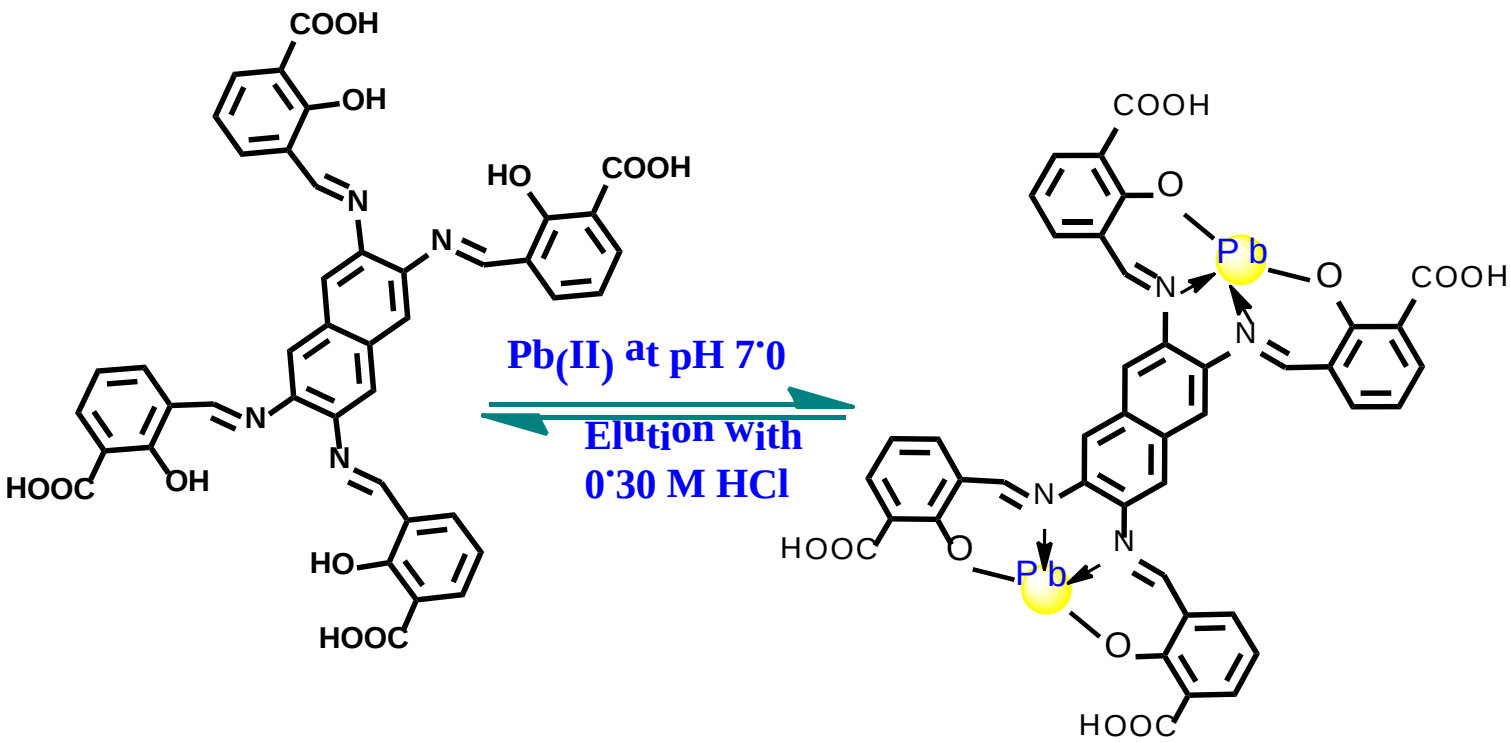

Scheme 2. The Pb(II) complexation mechanism with TSNT in optical detection and removal processes and also the elution operation with 0.30 M HCl acid.